The kinetics of transdermal ethanol exchange

Joseph C. Anderson[1] and Michael P. Hlastala[1,2]

Departments of [1]Medicine and [2]Physiology and Biophysics, University of Washington, Seattle, Washington

Anderson, Joseph C., and Michael P. Hlastala. The kinetics of transdermal ethanol exchange. *J Appl Physiol* 100: 649–655, 2006. First published October 20, 2005; doi:10.1152/japplphysiol.00927.2005.— The kinetics of ethanol transport from the blood to the skin surface are incompletely understood. We present a mathematical model to predict the transient exchange of ethanol across the skin while it is being absorbed from the gut and eliminated from the body. The model simulates the behavior of a commercial device that is used to estimate the blood alcohol concentration (BAC). During the elimination phase, the stratum corneum of the skin has a higher ethanol concentration than the blood. We studied the effect of varying the maximum BAC and the absorption rate from the gut on the relationship between BAC and equivalent concentration in the gas phase above the skin. The results showed that the ethanol concentration in the gas compartment always took longer to reach its maximum, had a lower maximum, and had a slower apparent elimination rate than the BAC. These effects increased as the maximum BAC increased. Our model's predictions are consistent with experimental data from the literature. We performed a sensitivity analysis (using Latin hypercube sampling) to identify and rank the importance of parameters. The analysis showed that outputs were sensitive to solubility and diffusivity within the stratum corneum, to stratum corneum thickness, and to the volume of gas in the sampling chamber above the skin. We conclude that ethanol transport through the skin is primarily governed by the washin and washout of ethanol through the stratum corneum. The dynamics can be highly variable from subject to subject because of variability in the physical properties of the stratum corneum.

diffusion; convection; blood alcohol concentration; skin alcohol; SCRAM

ACCURATE QUANTIFICATION OF alcohol concentration in the body is important in both forensic and physiological research applications. The most accurate and reliable method is direct blood sampling and analysis by gas chromatography. The alcohol breath test is commonly used because of its noninvasive and indirect approach. The measurement is not continuous, which makes it difficult to follow the pharmacokinetics of the blood alcohol concentration (BAC) and inaccurate due to the variability in delivery of the sample in different subjects (14).

The pharmacokinetics of alcohol are complex because of the intricate nature of the distribution into the various watery tissues in the body. The kinetics are dependent on absorption from the intestine into the blood, elimination from the blood via metabolism in the liver, and transport in different tissue compartments via diffusion and convection. This balance between absorption and elimination of alcohol is reflected in the BAC. After a drink, the BAC rises until absorption is complete. After a maximum in BAC is achieved, the BAC decreases during the "burn-off" or elimination phase primarily due to metabolism in the liver.

In legal cases involving the use of alcohol, courts may require abstinence until the matter is resolved in a legal proceeding. In the past, abstinence has been monitored with random breath testing, which leaves the possibility that a drinking event might be missed. The recent development of the SCRAM device (secure continuous remote alcohol monitor; Alcohol Monitoring Systems, Highlands Ranch, CO) (12) shows promise as a means for measuring a pseudocontinuous supradermal ethanol concentration, ethanol concentration in the gas space above the skin, at multiple points in time as a means for identification of violation of abstinence from alcohol. The SCRAM device is an ankle bracelet that simultaneously measures skin temperature and ethanol vapor above the skin surface. Ethanol arrives at the skin surface via passive alcohol diffusion from blood flowing through skin capillaries (insensible perspiration) and perspiration due to secretory activity of sweat glands (sensible perspiration). The alcohol concentration in an air sample taken from just above the skin surface vs. time is analyzed as a means of estimating BAC as a function of time. Only minimal information regarding the design and functional features of the SCRAM device is available in the literature. Thus we have chosen to focus on the kinetics of alcohol diffusion from the blood, through the skin, and into a generic measurement device lying on the surface of the skin.

It has been assumed that the shape of the supradermal ethanol concentration curve mimics the shape of the BAC curve. This interpretation may fail to recognize physiological variation in the process of diffusive transport through the skin, resulting in either false positive or false negative findings of alcohol consumption. This paper seeks to define the important factors governing the relationships between the BAC vs. time curve and the supradermal ethanol concentration vs. time curve. Additionally, this paper intends to evaluate the physiological limitations to interpretation of supradermal ethanol concentration data. In the present study, we develop a mathematical model of ethanol transport through the skin. Using this model, we explore how the time-varying concentration of ethanol in the blood affects the ethanol concentration above the skin. Additionally, a sensitivity analysis using Latin hypercube sampling (LHS) is implemented to reveal how variability in tissue, blood, and gas parameters affect skin ethanol concentration. These analyses answer the following two questions. Why is the supradermal ethanol concentration delayed and attenuated relative to the ethanol concentration in the blood? What factors are most responsible for this attenuation?

METHODS

Mathematical model. To simulate ethanol exchange across the skin surface, we chose a model consisting of four compartments: blood, epidermis, stratum corneum, and gas (Fig. 1). Dissolved ethanol in the

Address for reprint requests and other correspondence: J. C. Anderson, Division of Pulmonary and Critical Care Medicine, Box 356522, Univ. of Washington, Seattle, WA 98195-6522 (e-mail: clarkja@u.washington.edu).
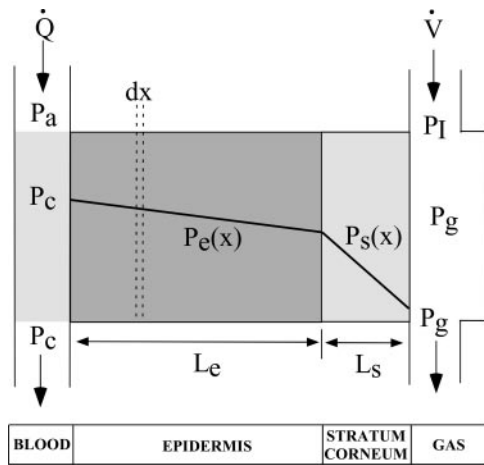
Fig. 1. Schematic showing a cross-section of skin next to a device for measuring supradermal ethanol concentration. Ethanol entering the system via the blood diffuses through the epidermis and stratum corneum before entering the gas compartment and is removed from the system by convective gas flow ($\dot{V}$). A differential length (dx) was used for mathematical analysis. Pa, Pc, P_e, P_g, P_s, arterial, capillary, epidermal, gas, and stratum corneum ethanol partial pressures, respectively. See Table 1 for more definitions.

blood is delivered to the skin via blood flow through the capillaries. Ethanol enters and leaves the capillaries at partial pressures Pa and Pc, respectively. Ethanol diffuses through the epidermis and the stratum corneum before it reaches the gas phase, which is ventilated with fresh air. As a first approach, we focused only on diffusional transport through the tissue layers. We neglected any transport resulting from sensible perspiration (i.e., sweating). We assumed that the capillary and gas compartments were individually well mixed and that uniform diffusion occurred across the epidermis and stratum corneum.

Similar to the model of vanLöbensels et al. (29), we used four coupled differential equations to describe mass transport between blood, epidermis, stratum corneum, and gas. *Equation 1* represents the rate of change of mass of a dissolved gas in the capillary blood compartment. It is equal to the rate of gas delivery to the capillary space via blood flow, the rate of gas removal via blood flowing out of the capillary, and the rate of diffusive gas flux across the capillary membrane into the epidermis. P_e is the partial pressure of ethanol in the epidermis. See Table 1 for parameter definitions.

$$\beta_b A_c L_c \frac{\partial Pc}{\partial t} = \dot{Q}\beta_b(Pa - Pc) - D_e\beta_e A_c \frac{\partial P_e}{\partial x}\bigg|_{x=0} \qquad (1)$$

Equations 2 and *3* describe diffusion in the epidermis and stratum corneum, respectively.

$$\beta_e A L_e \frac{\partial P_e}{\partial t} = D_e\beta_e A L_e \frac{\partial^2 P_e}{\partial x^2}, \quad 0 \le x < L_e \qquad (2)$$

$$\beta_s A L_s \frac{\partial P_s}{\partial t} = D_s\beta_s A L_s \frac{\partial^2 P_s}{\partial x^2}, \quad L_e < x \le L_e + L_s \qquad (3)$$

P_s is the partial pressure of ethanol in the stratum corneum. Between the epidermis and stratum corneum, we imposed that the flow of gas between the epidermis and stratum corneum was equal.

$$D_e\beta_e \frac{\partial P_e}{\partial x} = D_s\beta_s \frac{\partial P_s}{\partial x} \quad \text{at } x = L_e \qquad (4)$$

Equation 5 represents an enclosed air space above the skin. The rate of change of gas in this compartment is determined by addition of gas from the ambient air ($P_I = 0$), subtraction of gas removed by fresh air ventilation, and addition of gas diffusing across the air-skin interface from the stratum corneum, adjacent to the compartment.

$$\beta_g A L_g \frac{\partial P_g}{\partial t} = \dot{V}\beta_g(P_I - P_g) + D_s\beta_s A \frac{\partial P_s}{\partial x}\bigg|_{x=L_e+L_s} \qquad (5)$$

where P_g is the partial pressure of ethanol in the gas compartment. The section *Parameter estimates*, below, defines and presents average values for all model parameters.

We solved the system of four partial differential equations numerically to determine the partial pressure profiles in the epidermis and stratum corneum and the partial pressure of ethanol in the gas compartment as a function of time given a time-varying Pa of ethanol. Spatial derivatives were solved by upwind finite difference, and time derivatives were solved using LSODE, a time-integrating algorithm developed by Hindmarsh (13). The executable program was submitted as a batch job in which each simulation was solved numerically using an Intel Pentium IV computer running Digital Visual Fortran. Pc and Pg are equal to $P_e(0)$ and $P_s(L_e + L_s)$, respectively. To simplify the presentation of results, the partial pressures of ethanol in all model compartments were converted to equivalent BAC at 37°C using the following relationship:

$$BAC_{EQ} = \frac{\beta_b}{\beta_g RT} P \qquad (6)$$

where *R* is the universal gas constant (62,360 Torr·cm³·mol⁻¹·K⁻¹), T is the temperature (K), and β_g and β_b represent solubility (ml ethanol·100 ml medium⁻¹·Torr⁻¹) of ethanol in gas and blood, respectively.

Parameter estimates. We chose parameter values that corresponded to the average dimensions and physical characteristics of healthy skin tissue. The average values and uncertainty ranges for 11 parameters are listed in Table 1. We subjectively chose uncertainty ranges based on the methods used to select the average value. For example, little information is known about $\dot{V}$, but β_b was based on careful measurements. We assigned the former a high level of uncertainty ($\pm50\%$) and the latter a small level of uncertainty ($\pm10\%$). We assumed each variable to have a uniform (i.e., rectangular) probability distribution function, where the lower (upper) limit of the probability distribution function corresponded to the average value minus (plus) the uncertainty listed in Table 1. The skin tissue model has dimensions of 1 cm × 1 cm × L, where *L* is the thickness of each compartment. In our model, the skin tissue is composed of two compartments: the stratum corneum and the epidermis. The thickness of the stratum corneum ranges from 10 to 20 μm (3, 5, 18, 23, 24). On the basis of these data, we chose the thickness of the stratum corneum to be 15 μm (0.0015 cm). The thickness of the epidermis, the distance between the stratum corneum and the center of mass of the capillary vessels, depends on where the blood supply resides. Some investigators state the micro-

Table 1. *Model parameters and uncertainty ranges*

Symbol	Model Parameters	Average Value	Uncertainty, %
β_b	Solubility in blood*	232	± 10
β_e	Solubility in epidermis*	232	± 20
β_s	Solubility in stratum corneum*	211	± 25
D_e	Molecular diffusivity in epidermis, cm²/s	5.0×10^{-6}	± 25
D_s	Molecular diffusivity in stratum corneum, cm²/s	5.0×10^{-10}	± 50
L_e	Thickness of epidermis, cm	0.02	± 25
L_s	Thickness of stratum corneum, cm	0.0015	± 25
L_g	Thickness of gas compartment, cm	0.5	± 30
A_c	Capillary surface area, cm²	7.5×10^{-2}	± 50
$\dot{Q}$	Blood flow, ml/s	4.0×10^{-4}	± 30
$\dot{V}$	Convective gas flow, ml/s	5.0×10^{-5}	± 50

*Units for solubility are ml ethanol·100 ml medium⁻¹·Torr⁻¹.

circulation lies at a depth of 100–300 μm (9, 16, 20). Based on this data, we chose the thickness of the epidermis to be 200 μm (0.02 cm).

The capillary volume was calculated from estimates of the capillary diameter and surface area. We assumed the thickness of a capillary to be 7 μm (0.0007 cm), the diameter of a red blood cell. We estimated that the surface area of the capillaries covered 7.5% of the 1-cm^2 capillary-epidermis interface (0.075 cm^2) (26). Therefore, the capillary volume was 3.5×10^{-4} ml. The values for skin $\dot{Q}$ given in the literature range from 0.0057 to 0.049 ml·min^{-1}·cm^{-2} (2, 11, 25, 30). Based on these values, we assumed $\dot{Q}_s$ = 0.024 ml·min^{-1}·cm^{-2}. Therefore, $\dot{Q}$ in the model was 4.0×10^{-4} ml/s.

The volume of the gas compartment enclosed by the measurement device was estimated by assuming that the dimensions of the skin surface (*A*) were 1 cm × 1 cm = 1 cm^2 and the distance between the surface of the skin and the bottom of the detector was 0.5 cm. The corresponding gas volume (V_g) was 0.5 ml. Additionally, we assumed that the device measures ethanol once every 30 min and that each sample required 0.1 ml of gas. On average, over an entire 1 h, the flow rate within the gas compartment of the device would be 0.2 ml/h. To approximate this flow rate, we chose $\dot{V}$ = 5.0×10^{-5} ml/s.

The solubilities of ethanol in blood, epidermis, stratum corneum, and gas were obtained from experimental studies that reported liquid-air partition coefficients. For example, the partition coefficient of blood to air is the ratio of β_b to ethanol solubility in air, β_g. The "solubility" of ethanol in the gas phase, β_g, is defined as 0.132 ml ethanol·100 ml gas^{-1}·Torr^{-1} (17). The blood-air partition coefficient ($\lambda_{b:a}$) for ethanol is 1,756 at 37°C (15). Thus β_b = 1,756 × 0.132 = 232 ml ethanol·100 ml blood^{-1}·Torr^{-1}. We assumed the solubility of ethanol in the epidermis to be the same as that in blood, $\lambda_{b:e}$ = 1.0 (1, 25). On the basis of the stratum corneum-water partition coefficient (19, 21), $\lambda_{sc:w}$ = 0.75, and the water-air partition coefficient (15), $\lambda_{w:a}$ = 2,132 at 37°C, we estimated β_s to be = 0.75 × 2,132 × 0.132 = 211 ml ethanol·100 ml stratum corneum^{-1}·Torr^{-1}.

D_e of ethanol has been measured and found to range between 4×10^{-6} and 5.5×10^{-6} cm^2/s (10, 21). We chose $D_e = 5 \times 10^{-6}$ cm^2/s. Likewise, literature values of the D_s of ethanol ranges between 6.6×10^{-10} and 3.5×10^{-11} cm^2/s (21, 22). We chose $D_s = 5.0 \times 10^{-10}$ cm^2/s.

Model simulations. The model was used to simulate the elimination of ethanol from the blood through the skin and into the air. The time course of ethanol in the blood can be described by three parameters: absorption time, maximum BAC, and metabolic elimination rate. Ethanol was assumed to be absorbed, in a linear fashion, from the gut into the blood over a given period of time. We simulated absorption times ranging from 0.25 to 2.0 h in 0.25-h increments. At the end of the absorption phase, the concentration of ethanol in the blood reaches a peak. The maximum BAC (BAC_{max}) values used in these simulations range from 0.02 to 0.1 g/dl in 0.02 g/dl increments. In the postabsorptive state, BAC decreases predominantly as a result of metabolic breakdown. The rate of decrease in ethanol concentration in the blood (metabolic elimination rate) was assumed to be 0.018 g·dl^{-1}·h^{-1} for all simulations. For the gas compartment, we assumed that convective gas flow moves ambient air into the gas compartment to replace the gas that has been removed for measurement and that this ambient air does not contain ethanol (i.e., P_I = 0) for all simulations.

Using model simulations, we determined the effect of the absorption time and BAC_{max} on ethanol levels in and above the skin as a function of time. These simulations investigated all possible combinations of absorption time and BAC_{max} outlined above and used the average values of tissue thickness, molecular diffusivity, solubility, and flow rates provided in Table 1. Model simulations resulted in ethanol profiles in the blood, tissue, and air as a function of time. From these profiles, we calculated four quantities that describe the ethanol transport kinetics (Fig. 2): *1*) maximum ethanol concentration in the gas space ($C_{g,max}$) as calculated using *Eq. 6*, *2*) maximum decrease in ethanol concentration in the gas space with respect to time (WO_{max}), *3*) difference in time between the maximum ethanol concentration in
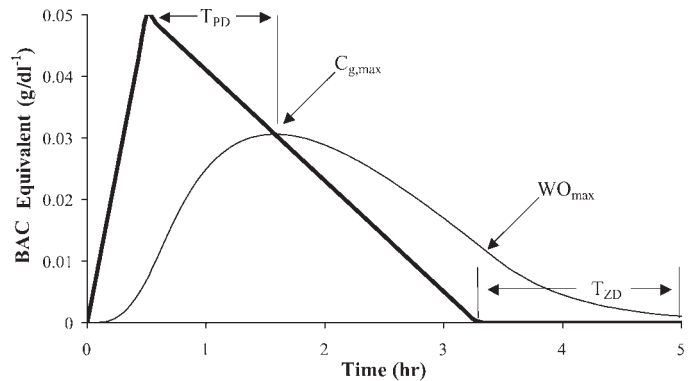

Fig. 2. Graphical definition of critical outputs. Blood alcohol concentration (BAC) curve (thick black line) was imposed, and the equivalent ethanol concentration in the gas compartment (C_g; thin black) was calculated from the model. The delay time between peaks (T_{PD}) is the difference in time between the maximum BAC and maximum ethanol concentration in the gas compartment ($C_{g,max}$). The maximum washout rate (WO_{max}) was calculated as the negative of the slope of the C_g curve. T_{ZD}, difference in time between zero ethanol concentration in the gas space and that in the blood.

the gas space and that in the blood (T_{PD}), and *4*) difference in time between zero ethanol concentration in the gas space and that in the blood (T_{ZD}). "Zero ethanol concentration in the gas space" was defined as a C_g = 0.001 g/dl.

Sensitivity analysis. We performed a sensitivity analysis of the mathematical model of transdermal ethanol transport to determine the relative importance of model parameters on critical model predictions. For this study, the LHS sensitivity analysis was chosen to investigate the relationship between model parameters and outputs (4). We evaluated the impact of 11 model parameters (Table 1) describing gas solubility, the tissue thickness, and molecular diffusion coefficients, on four outputs (Fig. 2). The following LHS sensitivity analyses were performed nine times using all combinations of the following conditions: *1*) absorption time of alcohol into the blood (0.5, 1, or 2 h) and *2*) maximum blood alcohol content as measured using the Widmark (31) formula (0.02, 0.05, or 0.10 g/dl).

To perform the LHS analysis, the mathematical model simulated the kinetics of ethanol transport through the skin as ethanol is absorbed into the blood and subsequently eliminated from the body. For each LHS analysis, the model simulated the transdermal kinetics of ethanol 50 times with each simulation involving a unique set of 11 parameter values. The value of each parameter during each of the 50 simulations was chosen by using the following algorithm. First, the probability distribution function for each parameter was divided into 50 equal probability intervals, the number of simulations. Second, each probability interval was assigned a number between 1 and 50, with 1 assigned to the probability interval nearest the lower confidence limit and 50 assigned to the probability interval nearest the upper confidence limit. Third, for every simulation, each parameter was assigned a random number between 1 and 50 without replacement (each number was used only once for a given parameter) that corresponded to the defined equal probability interval. Fourth, the equal probability interval corresponding to the random number was identified. The parameter value was equal to the average of the upper and lower limits of this interval. Thus a parameter value for each model simulation was chosen completely randomly (i.e., by random selection of the probability interval) but without replacement. Examples of studies using the LHS method for sensitivity analyses can be found in the literature (4, 7).

The last step in the sensitivity analysis was to determine a quantitative sensitivity index for each of the 11 parameters and establish a threshold to identify those parameters to which a particular output was sensitive. To do this, a partial rank correlation coefficient (PRCC) was
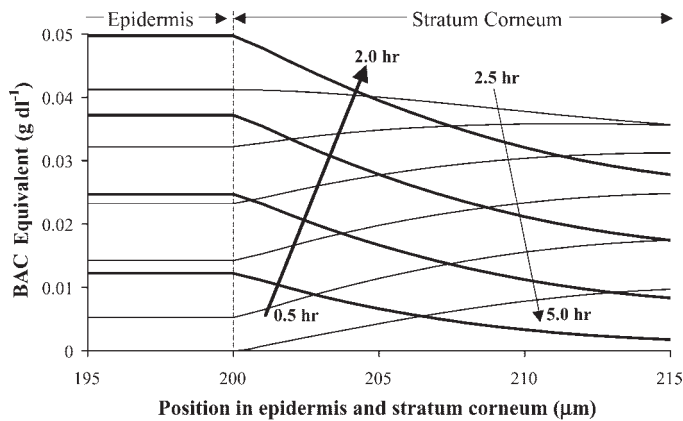
Fig. 3. Ethanol washin-washout kinetics in the tissue. BAC increases during the absorptive phase (solid lines), and ethanol follows the diffusion gradient from blood to tissue, loading the epidermis and stratum corneum with ethanol. BAC decreases during the postabsorptive phase (thin lines), the diffusion gradient reverses, and ethanol diffuses from the tissue into the blood. Tracings represent equivalent BAC vs. position at 0.5-h intervals. Model parameters are listed in Table 1. $BAC_{max} = 0.05$ g/dl, absorption time = 2 h, and metabolic elimination rate = 0.018 g·dl^{-1}·h^{-1}.

calculated for each input variable against each output variable (4). The significance of a nonzero PRCC value was tested using a two-sided Student's t-test (4) to determine whether each PRCC was statistically different from zero ($P < 0.05$). We studied the four outputs described in *Model simulations* ($C_{g,max}$, WO_{max}, T_{PD}, and T_{ZD}) with the sensitivity analysis.

RESULTS

Solutions of the model were well behaved with no instances of negative results or mass imbalance. Partial pressures at the boundaries between compartments were continuous. The numerically integrated time- and space-dependent solutions did not change as the size of the time step or spatial grid was altered.

Figure 3 demonstrates the spatial profiles of ethanol concentration through the epidermis and stratum corneum at multiple time points. The conditions imposed on the BAC profile are $BAC_{max} = 0.05$ g/dl, absorption time = 2 h, and metabolic elimination rate = 0.018 g·dl^{-1}·h^{-1}. For this simulation, the value for each model parameter is the average value listed in Table 1. Truncated ethanol profiles in the epidermis are presented because the equivalent BAC at the epidermis-stratum corneum interface (200 μm) is within 2% of the equivalent BAC at the blood-epidermis interface at all times. The ethanol profiles in the tissue are shown every 0.5 h. As BAC increases during absorption from the gut, the ethanol profiles (solid black line) in the stratum corneum increase as shown by the solid black arrow. Throughout the absorptive phase (solid black lines), BAC is always greater than the ethanol concentration in the gas phase because the large diffusion barrier imposed by the stratum corneum causes steep spatial gradients. After BAC reaches its peak (i.e., the rate of metabolic elimination is greater than that for absorption), the ethanol profiles in the stratum corneum (thin black line) decrease with time as shown by the thin black arrow. In the postabsorptive phase, the ethanol concentration in the blood drops below that in the gas phase because the metabolic elimination rate of ethanol in the liver is larger than the washout rate of ethanol from the stratum corneum. Therefore, the diffusion gradient reverses and ethanol diffuses from the tissue into the blood.

Devices measuring supradermal ethanol only sample ethanol in the gas space above the skin. Therefore, it is important to compare the concentration of supradermal ethanol, C_g, to the BAC at corresponding points in time. An example of a BAC and the corresponding C_g curve are presented in Fig. 2. This BAC curve (thick solid line) is a model input and has the following characteristics: a rise time of 30 min, a BAC_{max} of 0.05 g/dl, and a metabolic elimination rate of 0.018 g·dl^{-1}·h^{-1}. With this BAC curve and the typical model parameters (i.e., average values) listed in Table 1, the model simulated the transport of ethanol through the tissue and generated a typical C_g curve (thin solid curve) shown in Fig. 2. Compared with the BAC trace vs. time, the C_g curve has a maximum value, $C_{g,max}$, that is smaller and is delayed in time, T_{PD}, relative to BAC_{max} by ~1 h in this example. The decreasing slope of the C_g curve is less than that of the BAC curve. Thus the C_g curve is shifted, attenuated, and spread relative to the BAC curve. These transformations result from the diffusion barrier imposed by the stratum corneum.

We investigated how the shape of the BAC curve affected four outputs: $C_{g,max}$, WO_{max}, T_{PD}, and T_{ZD}. We imposed different BAC curves by changing BAC_{max} and the absorption time. The metabolic elimination rate was 0.018 g·dl^{-1}·h^{-1} for all simulations. We set each model parameter equal to the average value listed in Table 1. We plotted each output against BAC_{max} for eight different absorption times beginning with 0.25 h and ending with 2 h. Intermediate curves are separated by 0.25 h. Figure 4 shows the relationship between $C_{g,max}$ normalized by BAC_{max} and BAC_{max} for multiple absorption times. $C_{g,max}$ is directly related to absorption time and BAC_{max}. However, $C_{g,max}$ is at most equal to 78% of BAC_{max} and can be as small as 43% of BAC_{max} for a small absorption time and BAC_{max}. Figure 5 shows how WO_{max} changes with absorption time and BAC_{max}. For none of the simulations does the washout rate calculated from the C_g curve equal the imposed metabolic elimination rate of 0.018 g·dl^{-1}·h^{-1}. For any given absorption time and $BAC_{max} \geq 0.08$ g/dl, WO_{max} equals 0.0164 g·dl^{-1}·h^{-1}. For $BAC_{max} \leq 0.08$ g/dl, WO_{max} decreases with decreasing absorption time and BAC_{max}. For $BAC_{max} = 0.02$ and 0.25 h absorption times, WO_{max} is ~45%
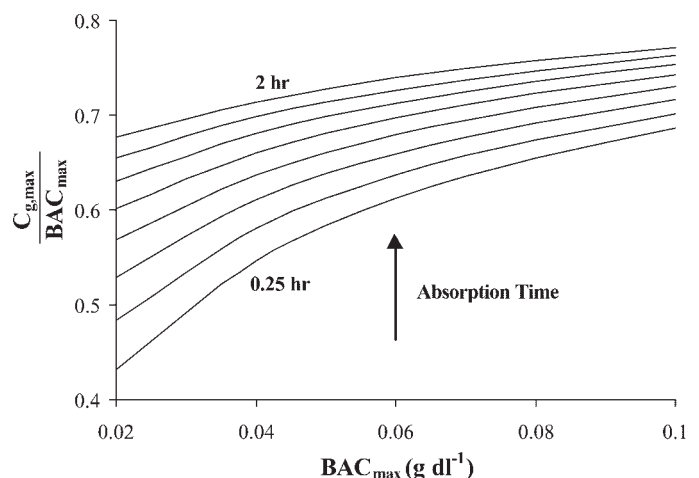

Fig. 4. $C_{g,max}$ normalized to BAC_{max} increases with BAC_{max} and absorption time. $C_{g,max}$ never equals BAC_{max}. *Top* and *bottom* curves represent 2- and 0.25-h absorption times, respectively, with curves interposed at 0.25-h increments.
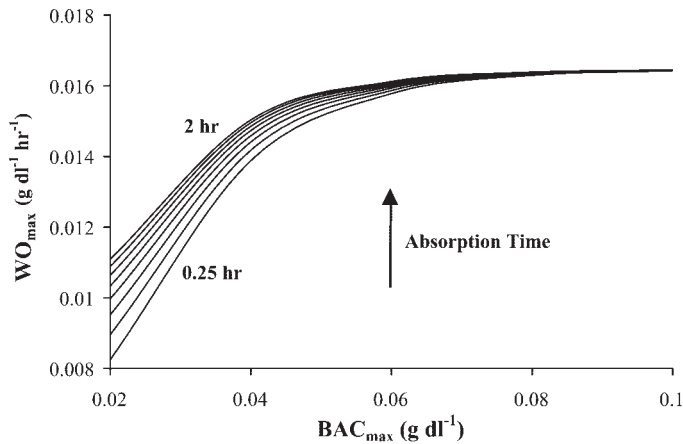
Fig. 5. WO_{max} increases with increases in BAC_{max} and absorption time. When $BAC_{max} \geq 0.08$ g/dl, $WO_{max} = 0.0164$ $g \cdot dl^{-1} \cdot h^{-1}$. *Top* and *bottom* curves represent 0.25- and 2-h absorption times, respectively, with curves interposed at 0.25-h increments. The metabolic elimination rate of ethanol in blood was 0.018 $g \cdot dl^{-1} \cdot h^{-1}$.

Fig. 7. T_{ZD} increases slightly with increases in BAC_{max} and absorption time. When $BAC_{max} \geq 0.08$ g/dl, $T_{ZD} = 3.3$ h. *Top* and *bottom* curves represent 2- and 0.25-h absorption times, respectively, with curves interposed at 0.25-h increments.

of the metabolic elimination rate. Because the WO_{max} is generally calculated at C_g values that are small, limitations of the measurement device may increase the difference between calculated WO_{max} and the metabolic elimination rate. Figure 6 shows that the time delay between BAC_{max} and $C_{g,max}$, T_{PD}, increases with increasing BAC_{max} and decreasing absorption time. The model predicts T_{PD} to range from 27 min for $BAC_{max} = 0.02$ and 2-h absorption time to 93 min for $BAC_{max} = 0.1$ and 15-min absorption time. Figure 7 shows the delay time between zeros, T_{ZD}, as a function of BAC_{max} and absorption time. For $BAC_{max} \leq 0.08$ g/dl, increasing BAC or absorption time increases T_{ZD}. However, for BAC ≥ 0.08 g/dl, $T_{ZD} = 3.3$ h independent of absorption time.

Nine sensitivity analyses were performed on the mathematical model using LHS. For a representative analysis with a 1-h absorption time and $BAC_{max} = 0.05$ g/dl, we present C_g curves resulting from the 50 simulations of the LHS analysis in Fig. 8 to show the effect of parameter uncertainty on C_g. For this LHS analysis, the PRCC and their corresponding P values are summa-
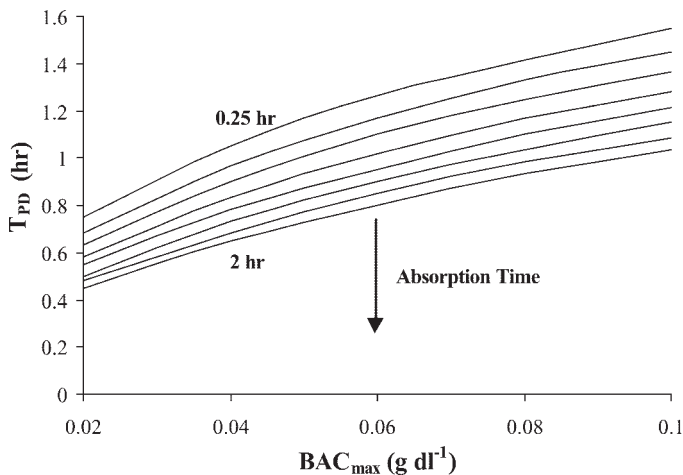
rized in Table 2. Coefficients with $P < 0.05$ are in bold. Although Table 2 presents sensitivity results for a representative BAC profile, this sensitivity relationship between outputs and parameters holds for all nine BAC curves studied. Additionally, three parameters ($\dot{V}$, β_e, and D_e) significantly affect WO_{max} under specific BAC_{max} conditions. WO_{max} is sensitive to gas flow when BAC_{max} is 0.1 or 0.05 g/dl and is sensitive to β_e and D_e when BAC_{max} is 0.05 or 0.02 g/dl.

There are four parameters to which all four outputs are statistically sensitive. One parameter defines the size of the gas compartment, L_g. The three remaining parameters, β_s, D_s, and L_s, together completely define the characteristics of the stratum corneum. Of these four parameters, two (D_s and L_s) have the largest absolute PRCC values. Therefore, variations in the value of these two parameters over their uncertainty range change the outputs more than alterations in any of the other parameters. The sign in front of the PRCC value indicates the relationship between a parameter and an output. A negative PRCC value signifies an inverse relationship; that is, an increase in the parameter will cause a decrease in the output. The

Fig. 6. T_{PD} between BAC_{max} and $C_{g,max}$ increases as BAC_{max} increases or the absorption time decreases. A 30- to 90-min delay exists between these 2 peaks for all cases shown. *Top* and *bottom* curves represent 0.25- and 2-h absorption times, respectively, with curves interposed at 0.25-h increments.
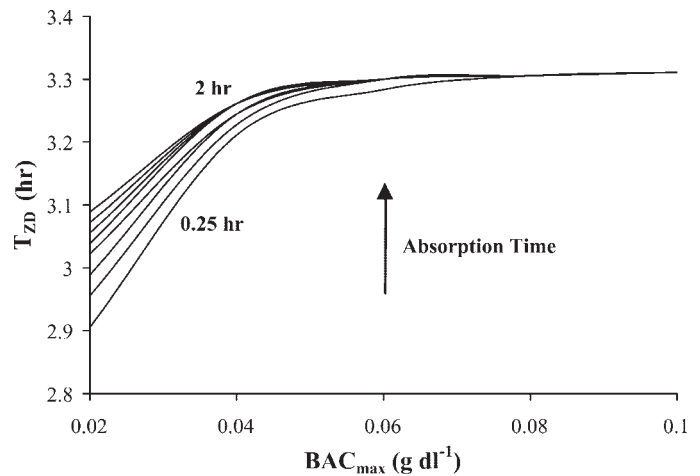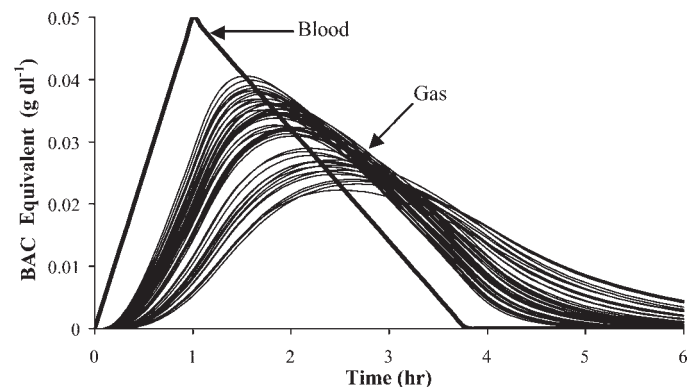

Fig. 8. Large variability in the supradermal ethanol curves results from relatively large uncertainty in the 11 model parameters. Fifty supradermal ethanol curves are predicted by the model. For each simulation, values for the 11 model parameters were selected using Latin hypercube sampling. BAC profile (thick black line) characteristics used for these simulations: ethanol absorption time = 1 h, $BAC_{max} = 0.05$ g/dl, and metabolic elimination rate for ethanol = 0.018 $g \cdot dl^{-1} \cdot h^{-1}$.

Table 2. *Sensitivity coefficients (PRCC) for a representative sensitivity analysis using a 1-h absorption time and BAC$_{max}$ = 0.05 g/dl*

| | Model Output | | | | | | | |
| | $C_{g,max}$ | | WO_{max} | | Peak delay (T_{PD}) | | End delay (T_{ZD}) | |
Variable	PRCC	P	PRCC	P	PRCC	P	PRCC	P
$\dot{V}$	**−0.632**	**0.001**	**−0.735***	**0.000**	0.096	0.486	−0.203	0.207
L_g	**−0.630**	**0.001**	**−0.572**	**0.003**	**0.495**	**0.000**	**0.665**	**0.000**
β_s	**0.681**	**0.000**	**0.681**	**0.000**	**−0.368**	**0.034**	**−0.398**	**0.024**
D_s	**0.974**	**0.000**	**0.967**	**0.000**	**−0.953**	**0.000**	**−0.964**	**0.000**
L_s	**−0.954**	**0.000**	**−0.933**	**0.000**	**0.949**	**0.000**	**0.952**	**0.000**
β_e	**0.284**	**0.024**	**0.258†**	**0.044**	−0.138	0.376	−0.219	0.176
D_e	0.095	0.494	**0.279†**	**0.027**	−0.148	0.344	−0.047	0.752
L_e	−0.065	0.665	−0.167	0.290	0.076	0.585	0.063	0.652
β_b	0.077	0.581	−0.010	0.947	0.065	0.645	−0.064	0.670
Q	−0.093	0.541	−0.119	0.439	0.051	0.719	0.063	0.655
A_c	0.077	0.582	0.070	0.615	0.110	0.423	0.019	0.897

PRCC, partial rank correlation coefficients. $C_{g,max}$, maximum ethanol concentration in the gas compartment; WO_{max}, maximum washout rate; T_{PD}, delay time between peaks; T_{ZD}, difference in time between zero ethanol concentration in the gas space and that in the blood. Values in boldface: $P < 0.05$. *Statistically significant when BAC$_{max}$ is 0.1 or 0.05 g/dl. †Statistically significant when BAC$_{max}$ is 0.05 or 0.02 g/dl.

parameters identified by this analysis may need to be more accurately measured or can be used to fit the model predictions to measured data.

DISCUSSION

To qualitatively validate our model, we compared our model predictions to experimental data from SCRAM-like devices in the literature that examined how changes in BAC$_{max}$ and absorption time from the gut affect C_g and C_g/BAC. First, the model predicted that $C_{g,max}$/BAC$_{max}$ was < 1 (i.e., $C_{g,max}$ was always less than BAC$_{max}$) and increases with absorption time and BAC$_{max}$ (Fig. 4). Experimental data show that $C_{g,max}$ is less than BAC$_{max}$ (as estimated with an alcohol breath test) (6, 27), and another study stated that the two peaks were "of similar amplitude" (28). An investigation (27) found $C_{g,max}$/BAC$_{max}$ resided between 0.29 and 0.5, whereas, in our model study, this ratio varied between 0.43 and 0.78. Second, the model predicted the delay time between $C_{g,max}$ and BAC$_{max}$ to be between 30 and 90 min. Three studies reported that T_{PD} was between 30 min and 2 h (6, 27, 28). Additionally, observations showed that T_{PD} increased from 30 to 120 min as BAC$_{max}$ increased from <0.1 g/dl to >0.15 g/dl (28). The model predicted the same trend between T_{PD} and BAC$_{max}$ (Fig. 6). Third, the model predicted that the maximum washout rate was always less than the imposed metabolic elimination rate of 0.018 g·dl^{-1}·h^{-1}. Experimental results (6) agree with this model prediction showing the elimination rate of ethanol in the gas phase to be 83% of that in the blood (as estimated with an alcohol breath test). Fourth, an experimental observation showed the delay time between C_g = 0 and BAC = 0 to be >2 h (28), which is similar to the model-predicted values (~3 h).

Our model included diffusion and neglected sensible perspiration (i.e., sweating). Whereas diffusion through the skin requires a significant amount of time for ethanol to cross the tissue and reach equilibrium, sensible perspiration moves liquid with an ethanol content similar to blood quickly (relative to diffusion) to the skin surface (27). If sensible perspiration was included in the model, the C_g curve would more closely match the BAC curve, causing T_{PD} to decrease and $C_{g,max}$ to more closely resemble BAC$_{max}$. However, our model results appear to underpredict T_{PD} and overpredict $C_{g,max}$ values measured experimentally and reported in the literature (see paragraph above), which indicates that perspiration is less important than diffusion and that the chosen parameter values (Table 1) are conservative estimates. A larger tissue thickness and smaller diffusion coefficients may be more appropriate. Although perspiration did not appear to impact the experimental data used for model validation, studies are needed to evaluate the effect of perspiration resulting from stressful conditions (e.g., exercise or hyperthermia) on ethanol transport through the skin.

A sensitivity analysis revealed the model to be most sensitive to parameters describing the stratum corneum (solubility, diffusivity, and thickness) and the gas compartment (thickness and convective gas flow). These parameters strongly influence the outputs for two reasons. First, the values of these parameters are less established, as reflected in their relatively large uncertainties that stem from large variability in their measurements (β_s, D_s, and L_s) or a lack of information ($\dot{V}$ and L_g). Second, these parameters significantly control the transport of ethanol or affect the measurement of ethanol. The stratum corneum provides the majority of resistance for transport of ethanol, as reflected in its large time constant. The stratum corneum has a larger time constant ($\tau_s = L_s^2/D_s = 3,380$ s) than the epidermis ($\tau_e = L_e^2/D_e = 80$ s) or the blood compartment ($\tau_b = $ capillary volume/$\dot{Q} = 1$ s). Experimental evidence supports this calculation. In an isolated skin preparation, investigators removed the stratum corneum and found the ethanol concentration above the skin increased by a factor of four compared with the intact preparation (8). However, the time constant in the gas phase is larger than all other compartments ($\tau = V_g/\dot{V} = 10,000$ s). The gas compartment's role is to collect ethanol for measurement, not to participate in ethanol transport. Thus the ideal time constant for the gas compartment would be infinity as $\dot{V}$ approaches 0 ml/s for any finite V_g.

Our sensitivity analysis demonstrates that the supradermal ethanol concentration is governed by the three model parameters describing the stratum corneum. In turn, each of these three parameters is dependent on water content and/or temperature. The thickness of the stratum corneum can increase almost fourfold from a dehydrated state ($L_s = 8.2$ μm) to a well-hydrated state

$(L_s = 27 \mu m)$ (21, 24). The molecular diffusivity of ethanol through this tissue can change by almost an order of magnitude from a value of 3.5×10^{-11} cm^2/s for a desiccated tissue to 6.6×10^{-10} cm^2/s for a well-hydrated stratum corneum (21, 22). Additionally, a temperature change from 30 to 37°C increases the molecular diffusivity of ethanol through water by 20% (32). Although stratum corneum is not water, this trend may still hold true except with a different magnitude of change. The solubility of ethanol in stratum corneum is dependent on water content. The solubility of ethanol in relatively dry stratum corneum was less than that in wet tissue (19, 21). Ethanol solubility in this tissue may decrease with temperature if it follows the behavior of ethanol solubility in water and blood (i.e., decreasing ~6% per °C) (15). Because these parameters significantly impact the predicted C_g curve, it may be necessary to control the water content and temperature of the tissue during experimental investigations.

The practice of using the skin alcohol monitoring device employs a single correction factor to adjust the peak gas concentration to an equivalent alcohol concentration in breath. Further correction to an equivalent alcohol concentration in blood is then required to allow use of skin alcohol readings to be compared with BACs. This practice is inherently flawed due to the large variation in supradermal gas concentration compared with blood concentration (as illustrated in Fig. 8). The variation in peak amplitude for supradermal gas is ~2 to 1. When this variation is coupled with the variation in breath to blood correction (14), it is clear that the measure of skin alcohol diffusion is plagued with an extremely large variation if the physiological variables are not accounted for in a quantitative manner.

Our mathematical model of ethanol transport across the skin during absorption from the gut and elimination from the body predicts *1*) ethanol kinetics follow classic washin-washout kinetics in the tissue, *2*) the supradermal ethanol concentration is attenuated and delayed compared with the BAC, *3*) ethanol transport through the skin is governed by the parameters describing the stratum corneum and the volume of gas above the skin, and *4*) the kinetics of ethanol transport can be highly variable between subjects because of variability in the physical characteristics of the stratum corneum. The results of this study suggest the water content and temperature of the stratum corneum along with the volume and flow rate of gas above the skin need to be closely controlled to ensure accurate measurements. Additional experimental information concerning the solubility of ethanol, diffusivity of ethanol through, and thickness of the stratum corneum and their dependence on temperature and water content is needed.

REFERENCES

1. **Anderson JC, Babb AL, and Hlastala MP.** Modeling soluble gas exchange in the airways and alveoli. *Ann Biomed Eng* 31: 1402–1422, 2003.
2. **Baumgardner JE, Graves DJ, Neufeld GR, and Quinn JA.** Gas flux through human skin: effect of temperature, stripping, and inspired tension. *J Appl Physiol* 58: 1536–1545, 1985.
3. **Blair C.** Morphology and thickness of the human stratum corneum. *Br J Dermatol* 80: 430–436, 1968.
4. **Blower SM and Dowlatabadi H.** Sensitivity and uncertainty analysis of complex models of disease transmission: an HIV model, as an example. *Int Stat Rev* 62: 229–243, 1994.
5. **Bronaugh RL, Stewart RF, and Congdon ER.** Methods for in vitro percutaneous absorption studies. II. Animal models for human skin. *Toxicol Appl Pharmacol* 62: 481–488, 1982.
6. **Brown DJ.** The pharmacokinetics of alcohol excretion in human perspiration. *Methods Find Exp Clin Pharmacol* 7: 539–544, 1985.
7. **Bui TD, Dabdub D, and George SC.** Modeling bronchial circulation with application to soluble gas exchange: description and sensitivity analysis. *J Appl Physiol* 84: 2070–2088, 1998.
8. **De Boer J, Plijter-Groendijk H, and Korf J.** Microdialysis probe for transcutaneous monitoring of ethanol and glucose in humans. *J Appl Physiol* 75: 2825–2830, 1993.
9. **Friend DR.** Transdermal delivery of contraceptives. *Crit Rev Ther Drug Carrier Syst* 7: 149–186, 1990.
10. **George SC, Babb AL, Deffebach ME, and Hlastala MP.** Diffusion of nonelectrolytes in the canine trachea: effect of tight junction. *J Appl Physiol* 80: 1687–1695, 1996.
11. **Gowrishankar TR, Stewart DA, Martin GT, and Weaver JC.** Transport lattice models of heat transport in skin with spatially heterogeneous, temperature-dependent perfusion. *Biomed Eng Online* 3: 42, 2004.
12. **Hawthorne JS, Phillips BK, Iiams ML, Roushey WJ, and Farmer NJ.** Method and apparatus for remote blood alcohol monitoring. In: *United States Patent Application Publication*. US patent no. 20040236199 Al, 2004 p. 33.
13. **Hindmarsh A.** *LSODE* (computer software). Livermore, CA: Lawrence Livermore Laboratory, 1981.
14. **Hlastala MP.** The alcohol breath test: a review. *J Appl Physiol* 84: 401–408, 1998.
15. **Jones AW.** Determination of liquid/air partition coefficients for dilute solutions of ethanol in water, whole blood, and plasma. *J Anal Toxicol* 7: 193–197, 1983.
16. **Pagliara A, Reist M, Geinoz S, Carrupt PA, and Testa B.** Evaluation and prediction of drug permeation. *J Pharm Pharmacol* 51: 1339–1357, 1999.
17. **Piiper J, Dejours P, Haab P, and Rahn H.** Concepts and basic quantities in gas exchange physiology. *Respir Physiol* 13: 292–304, 1971.
18. **Sato K, Sugibayashi K, and Morimoto Y.** Species differences in percutaneous absorption of nicorandil. *J Pharm Sci* 80: 104–107, 1991.
19. **Scheuplein RJ.** Mechanism of percutaneous adsorption. I. Routes of penetration and the influence of solubility. *J Invest Dermatol* 45: 334–346, 1965.
20. **Scheuplein RJ.** Permeability of the skin: a review of major concepts. *Curr Probl Dermatol* 7: 172–186, 1978.
21. **Scheuplein RJ and Blank IH.** Mechanism of percutaneous absorption. IV. Penetration of nonelectrolytes (alcohols) from aqueous solutions and from pure liquids. *J Invest Dermatol* 60: 286–296, 1973.
22. **Scheuplein RJ and Blank IH.** Permeability of the skin. *Physiol Rev* 51: 702–747, 1971.
23. **Schwindt DA, Wilhelm KP, and Maibach HI.** Water diffusion characteristics of human stratum corneum at different anatomical sites in vivo. *J Invest Dermatol* 111: 385–389, 1998.
24. **Scott RC, Corrigan MA, Smith F, and Mason H.** The influence of skin structure on permeability: an intersite and interspecies comparison with hydrophilic penetrants. *J Invest Dermatol* 96: 921–925, 1991.
25. **Shatkin JA and Brown HS.** Pharmacokinetics of the dermal route of exposure to volatile organic-chemicals in water—a computer-simulation model. *Environ Res* 56: 90–108, 1991.
26. **Stanton AW, Drysdale SB, Patel R, Mellor RH, Duff MJ, Levick JR, and Mortimer PS.** Expansion of microvascular bed and increased solute flux in human basal cell carcinoma in vivo, measured by fluorescein video angiography. *Cancer Res* 63: 3969–3979, 2003.
27. **Swift R.** Transdermal alcohol measurement for estimation of blood alcohol concentration. *Alcohol Clin Exp Res* 24: 422–423, 2000.
28. **Swift RM, Martin CS, Swette L, LaConti A, and Kackley N.** Studies on a wearable, electronic, transdermal alcohol sensor. *Alcohol Clin Exp Res* 16: 721–725, 1992.
29. **Mates vanLöbensels E, Anderson JC, Hildebrandt J, and Hlastala MP.** Modeling diffusion limitation of gas exchange in lungs containing perfluorocarbon. *J Appl Physiol* 86: 273–284, 1999.
30. **Whang JM, Quinn JA, Graves DJ, and Neufeld GR.** Permeation of inert gases through human skin: modeling the effect of skin blood flow. *J Appl Physiol* 67: 1670–1686, 1989.
31. **Widmark EMP.** *Principles and Applications of Medicolegal Alcohol Determination (Die theoretischen Grundlagen und die praktische Verwendbarkeit der gerichtlichmedizinischen Alkoholbestimmung, Berlin: 1932)*. Davis, CA: Biomedical Publications, 1981.
32. **Wilke CR and Chang P.** Correlation of diffusion coefficients in dilute solutions. *AICHE J* 1: 264–270, 1955.